



Contents lists available at ScienceDirect

Journal of Sound and Vibration

journal homepage: www.elsevier.com/locate/jsvi

Influences of imperfectness and inner constraints on an acoustic cloak with unideal pentamode materials

Yi Chen, Xiaoning Liu^{*}, Gengkai Hu

Key Laboratory of Dynamics and Control of Flight Vehicle, Ministry of Education, School of Aerospace Engineering, Beijing Institute of Technology, Beijing, 100081, China

ARTICLE INFO

Article history:

Received 2 January 2019
 Received in revised form 4 June 2019
 Accepted 6 June 2019
 Available online 10 June 2019

Keywords:

Pentamode acoustic cloak
 Shear resonance
 Damping
 Inner constraint
 Microstructure cloak
 Broadband

ABSTRACT

Pentamode materials are elastic solids with vanishing shear modulus, and can be used to cloak underwater sound with solid state and broadband advantages. However, pentamode materials produced with microstructures have inevitable small shear modulus. This paper systematically studies the effects of the shear rigidity and inner constraints on an acoustic cloak composing unideal pentamode materials. The shear rigidity introduces a new type of resonance in the radial direction, which is different from the traditional whispering-gallery resonance along the circumference. Totally fixed, radially fixed and free constraints on the inner surface are found to show significant differences in the cloaking function. To realize a broadband cloak with a suitable inner constraint in practice, we propose to attach a thin elastic shell on the inner surface to virtually tune the inner constraint. The strategy is validated with microstructure cloak simulation. This study will provide valuable guidance to facilitate practical applications of pentamode acoustic cloaks.

© 2019 Elsevier Ltd. All rights reserved.

1. Introduction

Invisibility cloak is the ultimate example of controlling wave propagation through material distributions, for which the transformation approach provides a general tool for identifying the required material parameters [1,2]. As for acoustics cloaks, meta-fluids with anisotropic densities were initially proposed following the same line as the transformation optics [3,4], namely the inertial cloak [5]. Various meta-fluids have been proposed with anisotropic densities such as alternating fluid layers [6], perforated plates [7] and resonant schemes [8,9]. However, these techniques require using fluids as the working media or they are limited to a narrow frequency band, and thus their engineering applications are limited. Furthermore, the achievable density anisotropy is quite small. The two principal densities can differ by five times for air sound [10], but only by two times for water sound [11]. Therefore, only the carpet cloaks [12,13] have been experimentally demonstrated since much higher anisotropy is required for omnidirectional cloaks.

Pentamode materials (PM) were proposed by Milton and Cherkaev in 1995 [14], as degenerate elastic solids with zero shear rigidity and achievable anisotropy in their moduli. These materials cannot resist shear deformation and they acoustically resemble ordinary fluids, although their moduli can be anisotropic. In 2008, Norris proved that PMs are also capable of controlling acoustic waves via the transformation method [5]. PMs can be approximated by solid materials after careful microstructural design to tune the shear rigidity. In contrast to many other metamaterials, the greatest advantages of PM are

^{*} Corresponding author.

E-mail address: liuxn@bit.edu.cn (X. Liu).

that, they are not resonance based and they are intrinsically broadband. Other advantages include sharper control due to their higher anisotropy and the solid nature of the controlling devices. These advantages have stimulated intensive recent researches into PMs, such as PM transformation theory [15,16], acoustic wave controlling applications [17–27], and PM microstructure design [28–34]. A cylindrical PM acoustic cloak with concrete microstructures was designed and numerically verified by Chen et al. [19], and was further experimentally tested in a two-dimensional (2D) waveguide to demonstrate its capability for manipulating underwater sound [26,35].

Several issues prevent a real cloak from being perfectly invisible over a broadband frequency range, e.g., the cloak is not mapped out from an infinitesimal point in the virtual space, the smooth gradient parameter of the cloak is discretized by piecewise layers, and the homogenization of the metamaterial is not accurate. For PM cloaks, an additional problem is that a practical solid-based PM cannot be ideal, i.e., with zero shear resistance, in order to be statically stable. In fact, a real PM belongs to the category of orthotropic solids. For example, the ratio of the shear relative to the bulk modulus is usually about 1% for a 2D PM [19], or about 1‰ for a three-dimensional PM [36], but not zero. The imperfectness of a PM is a particular issue because it induces a shear wave mode compared with a single longitudinal mode in an ideal PM. Numerical studies have shown that a real PM cloak exhibits discrete shear resonance instead of being broadband, as expected for an ideal PM [19]. Smith and Verrier [37] studied an acoustic cloak composing solids with anisotropic density and an isotropic modulus, and also found similar shear resonances. However, their investigations differed from the present study because we considered a PM with anisotropic modulus. The resonance can be suppressed by material damping but the cloak inner surface constraint is another important factor that influences the cloaking effect. In many previous studies [15,23,24], a radially fixed inner surface boundary was generally assumed to obtain the best invisibility. However, it should be noticed that, a radially fixed boundary is only reasonable for air sound because conventional solids such as a plastic or metal can be used as an acoustic rigid material. In terms of the elastic waves in PM cloaks, ordinary solids easily couple with the PMs and they barely fix the motion of the inner surface. From a practical perspective, the most realistic boundary for implementing underwater acoustic cloaks is the free inner surface. However, the free inner surface significantly influences the cloaking performance, as shown in this study, and a practical solution is still required to obtain invisibility. Due to the highly complex wave propagation in the gradient unideal PMs, most previous analyses treated PMs as ideal ones with zero shear rigidity [22,23], whereas few studies have considered the effects of the imperfectness of PMs and the inner constraint on acoustic cloaking.

In the present study, we derive a semi-analytical model of an acoustic cloak with unideal PMs and then systematically investigated the effects of the material parameters and inner constraint on the cloaking performance. The paper is organized as follows. In Section 2, we describe the PM and cylindrical cloak, and two parameters are introduced to quantify the imperfectness of an unideal PM. In Section 3, we derive an acoustic scattering solution for an acoustic cloak with unideal PMs. In Section 4, the impact of material parameters and inner constraints on the cloaking performance are investigated thoroughly. A practically feasible inner constraint is proposed to achieve broadband cloaking performance, which is verified based on microstructure cloak simulations. The concluding remarks are given in Section 5.

2. Characterization of pentamode materials and model of cylindrical cloaks

A PM is defined as an elastic material with five eigenvalues of its elasticity matrix being zero. Its elasticity tensor is simply written as $\mathbf{C} = \mathbf{K}\mathbf{S} \otimes \mathbf{S}$, where \mathbf{S} is the characteristic tensor. The stress in PMs is always proportional to the characteristic tensor $\boldsymbol{\sigma} = p\mathbf{S}$, where p is termed as the pseudo pressure. Ordinary fluids can be treated as PMs with isotropic characteristic tensors $\mathbf{S} = \mathbf{I}$. For a practically designed 2D PM, the elasticity matrix in the principal coordinates system is as follows [19],

$$\mathbf{C} = \begin{pmatrix} K_x & K_{xy} & 0 \\ K_{xy} & K_y & 0 \\ 0 & 0 & G_{xy} \end{pmatrix} \quad (1)$$

Two parameters for characterizing the degree of imperfectness can be defined as,

$$\nu = \frac{|K_{xy}|}{\sqrt{K_x K_y}} \quad \mu = \frac{G_{xy}}{\sqrt{K_x K_y}} \quad (2)$$

To approximate a perfect PM, the conditions $|\nu - 1| \ll 1$ and $\mu \ll 1$ should both be satisfied. For the isotropic case, a single condition that $\nu \ll 1$ is sufficient since $\nu = 1 - 2\mu$. For anisotropic materials, both ν and μ should be restricted.

The material parameters for a PM cloak can be derived from transformation theory as shown in Fig. 1 [5]. First, we suppose that a virtual space Ω & Ω^{out} is occupied by a homogenous fluid with density ρ_0 and modulus K_0 . Secondly, by coordinate mapping $\mathbf{x} = f^{-1}(\mathbf{X})$, we can map the acoustic equation for ordinary fluids in Ω onto the acoustic equation in ω for PMs. Then, the acoustic wave propagating along a straight trajectory in the virtual space will propagate along a curved trajectory and the central region in the physical space becomes undetectable. The PM parameters required for the cloak are [5],

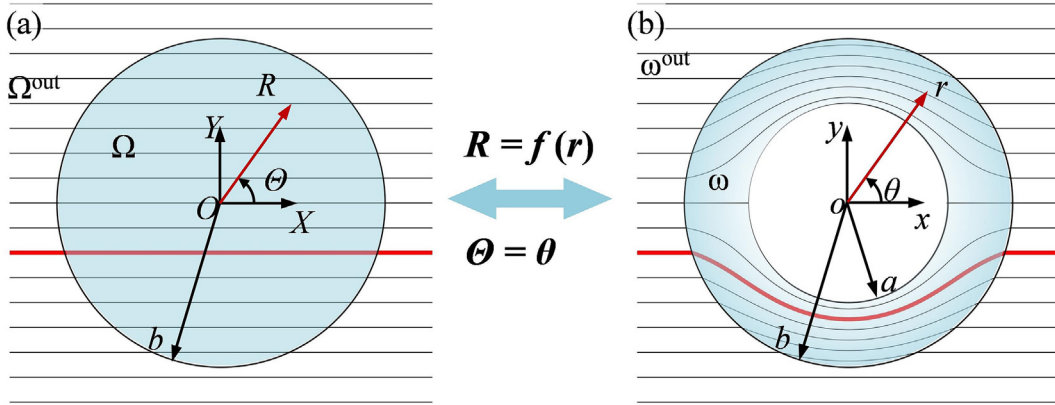


Fig. 1. Illustration of the transformation approach for a pentamode cloak; (a) Virtual space with region Ω^{out} and Ω ; (b) Physical space with background region ω^{out} and cloak region ω , where Ω and ω have the same outer boundary.

$$\rho' = \rho' \mathbf{I}, \quad \mathbf{C} = \begin{pmatrix} K_r & \sqrt{K_r K_\theta} & 0 \\ \sqrt{K_r K_\theta} & K_\theta & 0 \\ 0 & 0 & 0 \end{pmatrix} \quad (3)$$

$$\rho' = \rho_0 \frac{f(r)f'(r)}{r}, \quad K_r = K_0 \frac{f(r)}{rf'(r)}, \quad K_\theta = K_0 \frac{rf'(r)}{f(r)} \quad (4)$$

where K_r and K_θ are the principal moduli along the radial and circumferential directions, respectively. Different functions $f(r)$ can be used to simplify the material parameters provided that $f(b) = b$ and $f(a) = \delta$. A small radius $\delta \ll 1$ is employed in the present study in order to avoid material singularity near the inner boundary. The commonly used functions $f(r)$ that leads to a uniform density or modulus can be unified as follows,

$$f(r) = \left(\frac{b^n - \delta^n}{b^n - a^n} r^n - \frac{a^n - \delta^n}{b^n - a^n} b^n \right)^{1/n} \quad (5)$$

The linear mapping, uniform density mapping and uniform modulus mapping can be obtained by taking n to be 1, 2 and $+\infty$, respectively.

3. Scattering of an acoustic cloak with imperfect pentamode materials

In this section, we consider the scattering of a cylindrical cloak with imperfect PMs, i.e., essentially an orthotropic solid shell with gradient density $\rho(r)$ and modulus $\mathbf{C}(r)$, where the principal axis is aligned with the polar frame. A closed form solution for the acoustic scattering of a cylindrical orthotropic solid shell is very tedious to obtain, if not impossible. Thus, we employ the state space approach, which is traditionally used for laminated orthotropic plates [38,39]. The continuous cloak is first discretized into N layers (Fig. 2), where each layer is sufficiently thin because of the reasons explained in the following. The j th pentamode layer enclosed by radius r_{j-1} and r_j is treated as homogenous with density $\rho_j = \rho_j((r_{j-1} + r_j)/2)$ and modulus $\mathbf{C}_j = \mathbf{C}_j((r_{j-1} + r_j)/2)$. The domain outside the cloak is filled with a homogeneous fluid (ρ_0, K_0), and it is denoted as the $(N + 1)^{\text{th}}$ layer.

We consider a plane wave with frequency ω incidents from the left, $p_{\text{in}} = \exp(ik_0x)$, and the incident plane wave can be decomposed as,

$$p_{\text{in}} = \sum_{n=0}^{\infty} a_n J_n(k_0 r) \cos n\theta \quad (6)$$

where the time dependence term $\exp(-i\omega t)$ is omitted as convention, $k_0 = \omega/c_0$ is the wave number, $c_0 = (K_0/\rho_0)^{1/2}$ is the wave speed and $J_n(k_0 r)$ is the n th order Bessel function. The incident coefficient is $a_n = (2 - \delta_{0n})i^n$ ($n > 0$), where δ represents the Kronecker delta. The scattered pressure p_{sc} in the background fluid is governed by $\nabla^2 p_{\text{sc}} + (k_0)^2 p_{\text{sc}} = 0$, and it follows the decompositions,

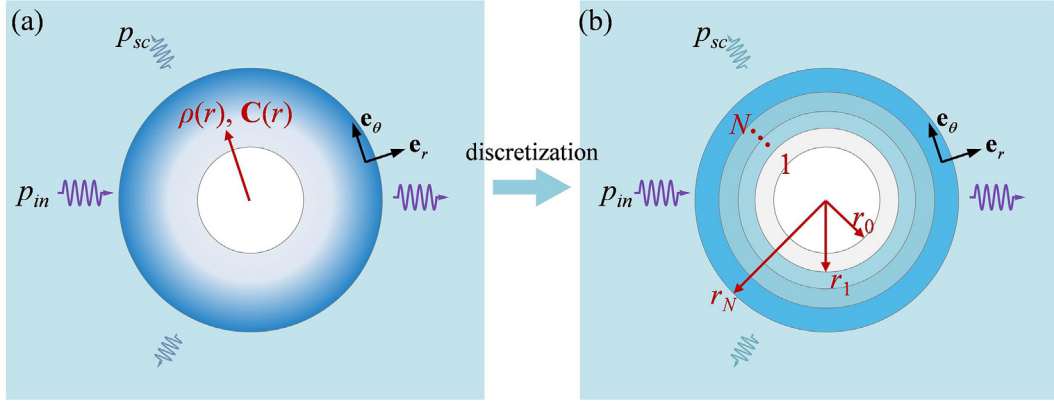


Fig. 2. Scattering model of a pentamode cloak; (a) A cloak with smoothly varying pentamode materials is discretized into (b) a cloak with N layers of homogeneous material.

$$p_{sc} = \sum_{n=0}^{\infty} b_n H_n^{(1)}(k_0 r) \cos n\theta \quad (7)$$

where b_n is the unknown n th order scattering coefficient and $H_n^{(1)}(k_0 r)$ is the n th order Hankel function of the first kind. Wave propagation in the PMs should be considered to solve the scattering coefficient. For the j th layer, the constitutive, geometry and momentum equations can be expressed in the polar coordinates as,

$$\begin{pmatrix} \sigma_{jr} \\ \sigma_{j\theta} \\ \sigma_{jr\theta} \end{pmatrix} = \begin{pmatrix} K_{jr} & K_{jr\theta} & 0 \\ K_{jr\theta} & K_{j\theta} & 0 \\ 0 & 0 & G_{jr\theta} \end{pmatrix} \begin{pmatrix} \varepsilon_{jr} \\ \varepsilon_{j\theta} \\ 2\varepsilon_{jr\theta} \end{pmatrix} \quad (8)$$

$$\varepsilon_{jr} = \frac{\partial u_{jr}}{\partial r}, \quad \varepsilon_{j\theta} = \frac{1}{r} \frac{\partial u_{j\theta}}{\partial \theta} + \frac{u_{jr}}{r}, \quad \varepsilon_{jr\theta} = \frac{1}{2} \left(\frac{\partial u_{j\theta}}{\partial r} + \frac{1}{r} \frac{\partial u_{jr}}{\partial \theta} - \frac{u_{j\theta}}{r} \right) \quad (9)$$

$$\frac{\partial \sigma_{jr}}{\partial r} + \frac{1}{r} \frac{\partial \sigma_{jr\theta}}{\partial \theta} + \frac{\sigma_{jr} - \sigma_{j\theta}}{r} = -\rho_j \omega^2 u_{jr}, \quad \frac{\partial \sigma_{jr\theta}}{\partial r} + \frac{1}{r} \frac{\partial \sigma_{j\theta}}{\partial \theta} + \frac{2\sigma_{jr\theta}}{r} = -\rho_j \omega^2 u_{j\theta} \quad (10)$$

where K_{jr} , $K_{j\theta}$ and $G_{jr\theta}$ are the moduli of the j th layer, ε_{jr} , $\varepsilon_{j\theta}$ and $\varepsilon_{jr\theta}$ are the strains, and σ_{jr} , $\sigma_{j\theta}$ and $\sigma_{jr\theta}$ are the stresses. Considering the orthogonality of the different scattering modes and the continuity at the fluid–PM interface, the following ansatz are employed for the displacements and stresses,

$$u_{jr} = \sum_{n=0}^{\infty} u_{jnr}(r) \cos n\theta, \quad u_{j\theta} = \sum_{n=0}^{\infty} u_{jn\theta}(r) \sin n\theta \quad (11)$$

$$\sigma_{jr} = \sum_{n=0}^{\infty} \sigma_{jnr}(r) \cos n\theta, \quad \sigma_{jr\theta} = \sum_{n=0}^{\infty} \sigma_{jnr\theta}(r) \sin n\theta, \quad \sigma_{j\theta} = \sum_{n=0}^{\infty} \sigma_{jn\theta}(r) \cos n\theta \quad (12)$$

where $(u_{jnr}, u_{jn\theta})$ and $(\sigma_{jnr}, \sigma_{jnr\theta}, \sigma_{jn\theta})$ are denoted as the n th order displacement and stress of the j th layer in polar coordinates, respectively. To consider the continuity at the interface between adjacent pentamode layers, the n th order state space vector is defined as follows,

$$\mathbf{D}_{jn}(r) = \{u_{jnr}(r), u_{jn\theta}(r), \sigma_{jnr}(r), \sigma_{jnr\theta}(r)\}^T \quad (13)$$

By substituting the mode expansions in Eq. (11) and Eq. (12) into Eq. (10), we can derive an ordinary differential equation for the n th order state space vector of the j th layer

$$\frac{d}{dr} \mathbf{D}_{jn}(r) = \mathbf{P}_{jn}(r) \mathbf{D}_{jn}(r) \quad (14)$$

where the matrix $\mathbf{P}_{jn}(r)$ is,

$$\mathbf{P}_{jn}(r) = \begin{pmatrix} \frac{1}{r} \frac{K_{jr\theta}}{K_{jr}} & \frac{n}{r} \frac{K_{jr\theta}}{K_{jr}} & \frac{1}{K_{jr}} & 0 \\ \frac{n}{r} & \frac{1}{r} & 0 & \frac{1}{G_{jr\theta}} \\ \frac{1}{r^2} \xi_j - \rho_j \omega^2 & \frac{n}{r^2} \xi_j & \frac{1}{r} \left(\frac{K_{jr\theta}}{K_{jr}} - 1 \right) & -\frac{n}{r} \\ \frac{n}{r^2} \xi_j & \frac{n}{r^2} \xi_j - \rho_j \omega^2 & \frac{n}{r} \frac{K_{jr\theta}}{K_{jr}} & -\frac{2}{r} \end{pmatrix} \tag{15}$$

and $\xi_j = (K_{jr}K_{j\theta} - (K_{jr\theta})^2)/K_{jr}$. Based on the operation given above, the original second order partial differential equation is transformed into a more readily handled ordinary differential equation. The j th PM layer is homogeneous but Eq. (14) cannot be solved explicitly since $\mathbf{P}_{jn}(r)$ varies according to position r . Thus, we discretize the cloak into sufficiently thin layers such that $\mathbf{P}_{jn}(r)$ can be regarded as a constant matrix evaluated at the midpoint. As a consequence, Eq. (14) admits an exponential solution, and the state space vectors at the front and back surface of the j th PM layer are related as follows,

$$\mathbf{D}_{jn}(r_j) = \exp\left((r_j - r_{j-1})\mathbf{P}_{jn}\left(\frac{r_{j-1} + r_j}{2}\right)\right)\mathbf{D}_{jn}(r_{j-1}) \tag{16}$$

Due to the continuity of the state space vector at the interface between adjacent PM layers, i.e., $\mathbf{D}_{jn}(r_{j-1}) = \mathbf{D}_{(j-1)n}(r_{j-1})$, the state space vector at the outer surface of cloak, $\mathbf{D}_{Nn}(r_N)$, depend on that of the innermost surface, $\mathbf{D}_{1n}(r_0)$, according to the following transmittance relationship,

$$\mathbf{D}_{Nn}(r_N) = \mathbf{T}_n \mathbf{D}_{1n}(r_0), \quad \mathbf{T}_n = \prod_{j=1}^{j=N} \exp\left((r_j - r_{j-1})\mathbf{P}_{jn}\left(\frac{r_{j-1} + r_j}{2}\right)\right) \tag{17}$$

To solve the scattering coefficient b_n and the state space vectors \mathbf{D}_{1n} and \mathbf{D}_{Nn} , Eq. (17) must be complemented with a set of continuity conditions at the fluid–PM interface,

$$u_{Nnr}(r_N) = \frac{1}{\rho_0 \omega^2} \left(a_n J'_n(k_0 r_N) + b_n H_n^{(1)'}(k_0 r_N) \right) \tag{18}$$

$$\sigma_{Nnr}(r_N) = - \left(a_n J_n(k_0 r_N) + b_n H_n^{(1)}(k_0 r_N) \right), \quad \sigma_{Nnr\theta}(r_N) = 0 \tag{19}$$

and the constraint on the cloak's inner surface. Three common constraints can be applied, as follows.

$$u_{1nr}(r_0) = 0, \quad u_{1n\theta}(r_0) = 0 \quad \text{for totally fixed case} \tag{20}$$

$$u_{1nr}(r_0) = 0, \quad \sigma_{1nr\theta}(r_0) = 0 \quad \text{for radially fixed case} \tag{21}$$

$$\sigma_{1nr}(r_0) = 0, \quad \sigma_{1nr\theta}(r_0) = 0 \quad \text{for free case} \tag{22}$$

After some algebra, the scattering coefficient can be expressed in compact form as,

$$b_n = - a_n \frac{J'_n(k_0 r_N) - \rho_0 \omega^2 J_n(k_0 r_N) \chi}{H_n^{(1)'}(k_0 r_N) - \rho_0 \omega^2 H_n^{(1)}(k_0 r_N) \chi} \tag{23}$$

where the factor χ is,

$$\chi = \frac{T_{n13}T_{n44} - T_{n14}T_{n43}}{T_{n34}T_{n43} - T_{n33}T_{n44}} \quad \text{for totally fixed case} \tag{24}$$

$$\chi = \frac{T_{n12}T_{n43} - T_{n13}T_{n42}}{T_{n33}T_{n42} - T_{n32}T_{n43}} \quad \text{for radially fixed case and} \tag{25}$$

$$\chi = \frac{T_{n11}T_{n42} - T_{n12}T_{n41}}{T_{n32}T_{n41} - T_{n31}T_{n42}} \quad \text{for free case} \tag{26}$$

In the equations above, T_{nij} ($i, j = 1-4$) represent the elements of the transmittance matrix T_n . Using the asymptotic expansion of the Hankel function, the scattered pressure in the far field can be approximated as,

$$p_{sc} \approx A(\theta)r^{-1/2} \exp(ik_0r), \quad A(\theta) = \sum_{n=0}^{\infty} b_n \sqrt{\frac{2}{\pi k_0}} \exp\left(-i\left(\frac{n\pi}{2} + \frac{\pi}{4}\right)\right) \cos n\theta \quad (27)$$

where $A(\theta)$ is the form function of the scattered pressure, and the parameter θ is the azimuth angle, and $A(0)$ and $A(\pi)$ are the forward and backward scattering coefficients, respectively. In order to quantitatively assess the cloaking performance, we use the total scattering cross section (TSCS), which accounts for the scattering in all directions [19,40]. The TSCS is defined as the ratio between the scattered energy and incident energy on the cloak inner cross-section, which can be expressed in terms of the scattering coefficients,

$$\sigma_{tot} = \frac{E_{sc}}{E_{in}} = \frac{1}{k_0 r_0} \sum_{n=0}^{\infty} (1 + \delta_{0n}) |b_n|^2 \quad (28)$$

It should be noticed that the scattering coefficient of each order contributes to the TSCS and the cloak is perfectly invisible only if the entire scattering coefficient vanishes.

4. Results and discussions

4.1. Shear resonance and its effects in the TSCS spectrum

We consider a pentamode cloak with the parameters derived from the transformation method given above. The cloak's inner and outer radii are treated as a and $b = 2a$, and the small parameter is set as $\delta = a/5$. The density ρ , and moduli K_r and K_θ in the cloak are obtained from Eq. (4) using the uniform density mapping, and $K_{r\theta}$ and $G_{r\theta}$ are deduced from the PM characteristic parameters, i.e., $K_{r\theta} = \nu(K_r K_\theta)^{1/2}$ and $G_{r\theta} = \mu(K_r K_\theta)^{1/2}$. The imperfectness of PM is assumed to be $\nu = 0.99$ and $\mu = 0.01$. Other choices for δ and the mapping function will not affect the main conclusion. The inner surface of the cloak is assumed to be totally fixed, and the effects of different constraints are addressed next. In total, 21 orders of Bessel functions are included in the theoretical calculation.

The theoretically calculated TSCS and first four orders of the scattering amplitudes $|b_n|$ are shown in Fig. 3(a) (b). Compared with a bare rigid scatter, the TSCS for the cloaked case decreases significantly at most frequencies. However, sharp peaks are also observed in the TSCS, and they are attributed to shear resonance due to the nontrivial shear modulus [19]. It should be noted that these shear resonances are quite different from the whispering-gallery resonances in cylinder objects, which are coupled longitudinal and shear modes, and they occur at rather high frequencies [41,42]. These resonances occur when the circumference is almost an integer multiple of the wavelength. Fig. 3(f) depicts the resonance displacements in a steel cylinder immersed in water, which shows that the displacements are nearly periodic along the θ -direction and concentrated at the outer boundary. By contrast, the shear resonances in the PM cloak exhibited shear waves along the radial direction

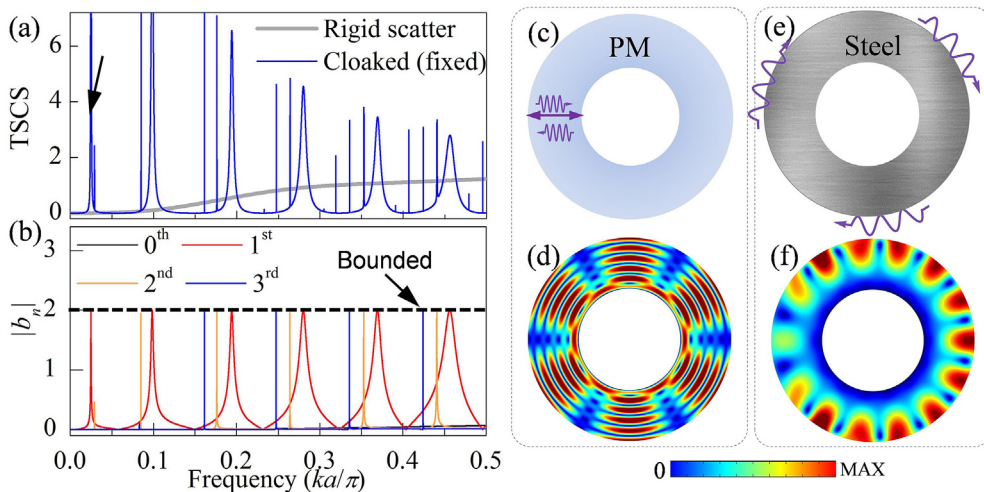


Fig. 3. (a) TSCS for a rigid scatter and PM cloak with a totally fixed inner surface; (b) Scattering coefficient amplitude corresponding to the first four orders; (c) Resonance in the PM cloak formed by shear waves along the radial direction; (d) Resonant displacements in the PM cloak. (e) Resonance in ordinary solids formed by whispering-gallery wave along the circumferential direction; (f) Resonant displacements in a steel shell.

(Fig. 3(c)), and the displacement dominated over the whole cloak (Fig. 3(d)). The resonances occurred when the shear waves travelling back and forth along the radial direction change phase by an integer multiple of 2π . In addition, different inner constraints change the resonance frequencies. Due to the resonance mechanism above, adjacent resonance frequencies of the same order differ by $\Delta(ka/\pi) = c_T/c_0$, where c_T is the shear wave speed in the PM. The resonance spacing is approximately $\Delta(ka/\pi) \approx 0.0867$, which agrees fairly well with the numerical results. Another difference in the shear resonances compared with the conventional whispering-gallery resonance is that it can occur at an extremely low frequency. For instance, at the first resonance frequency (Fig. 3(a)), the wavelength in the background fluid is much larger than the cloak dimension $\lambda \approx 81a$. The low frequency resonance is determined by the small shear modulus.

It is also interesting that although the resonance peaks of the scattering coefficients are very sharp, they are always bounded $|b_n| < |a_n| \leq (2 - \delta_{0n})$. From a physical perspective, wave modes of different orders are not coupled due to the circular shape of the cloak, and thus each scattering amplitude $|b_n|$ is bounded by the incident amplitude $|a_n|$ of the same order, otherwise, the scattering amplitude can be much higher than the incident amplitude if the cloak has an irregular inner or outer boundary. The bounded scattering amplitude can also be explained theoretically as follows. At the outer surface $r = r_N$ of the PM cloak, we define the n th order effective surface acoustic impedance,

$$Z_n(k_0) = \frac{p_{nr}(r_N)}{v_{nr}(r_N)} \quad (29)$$

where $v_{nr}(r_N)$ and $p_{nr}(r_N)$ denote the n th order velocity and pressure, respectively, of the background fluid at $r = r_N$. Due to the continuity condition at the outer surface of the cloak, the effective surface impedance $Z_n(k_0)$ can be determined from the transmittance matrix Eq. (17). For instance, with a radially fixed boundary, $Z_n(k_0)$ can be written as,

$$Z_n(k_0) = \frac{i}{\omega} \frac{1}{\chi_1} = -\frac{i}{\omega} \frac{T_{n32}T_{n43} - T_{n33}T_{n42}}{T_{n12}T_{n43} - T_{n13}T_{n42}} \quad (30)$$

The transmittance matrix is always real valued and the effective impedance is imaginary valued. By substituting the pressure and velocity of the background fluid into Eq. (29), we can obtain the scattering coefficient,

$$b_n = -a_n \frac{k_0 J_n(k_0 r_N) - \xi(k_0) J'_n(k_0 r_N)}{k_0 H_n^{(1)}(k_0 r_N) - \xi(k_0) H_n^{(1)'}(k_0 r_N)}, \quad \xi_n(k_0) = \frac{Z_n(k_0)}{i\rho_0 c_0} \quad (31)$$

where, the impedance ratio $\xi_n(k_0)$ is real valued. The solution given above can recover the classical result for rigid or soft scatter. For a rigid scatter, the surface impedance is infinitely large $\xi(k_0) = \infty$ since the surface velocity is zero, whereas a soft scatter implies a zero impedance $\xi(k_0) = 0$ because the surface pressure is enforced to be zero. Given the identity $J_n(kr) Y'_n(kr) - J'_n(kr) Y_n(kr) = 2/(\pi r)$, where $Y_n(x)$ represents the Bessel function of the second kind, then the denominator in Eq. (31) cannot be exactly zero. Thus we can conclude that the scattering coefficients are always bounded

$$|b_n| = \left| -a_n \frac{k_0 J_n(k_0 r_N) - \xi(k_0) J'_n(k_0 r_N)}{(k_0 J_n(k_0 r_N) - \xi(k_0) J'_n(k_0 r_N)) + i(k_0 Y_n(k_0 r_N) - \xi(k_0) Y'_n(k_0 r_N))} \right| \leq |a_n| \quad (32)$$

Equation (32) is not only valid for PM cloaks, and the derivation implies that for any cylindrical object, the acoustic scattering amplitude $|b_n|$ cannot exceed the incident amplitude $|a_n|$ of the same order. According to Eq. (31), the n th order resonance occurs when the imaginary part of the denominator is almost zero or very small,

$$k_0 Y_n(k_0 r_N) - \xi(k_0) Y'_n(k_0 r_N) \approx 0 \quad (33)$$

Similarly, the minimal scattering amplitude $b_n \approx 0$ for the n th order is obtained when the numerator in Eq. (31) is nearly zero $k_0 J_n(kr) - \xi(k_0) J'_n(kr) \approx 0$. The extremely small scattering can be understood as an anti-resonance phenomenon, which may be exploited to enhance the cloaking effect for a specific incident order.

4.2. Effects of material damping and inner constraint

Next, we investigate the impacts of material damping and the inner constraints on the cloaking performance. In order to suppress the resonance, it is natural to introduce material damping, which can be implemented in practice by filling the PM structures with absorbing materials or by using lossy base materials. For illustrative purposes, the PM material is assumed to be lossy. In particular, the moduli of the cloak material are multiplied by $1 + 0.005i$. The TSCS for the damped cloak is shown in Fig. 4(a), which demonstrates that the narrow peaks are significantly suppressed, except for the wide peaks corresponding to the first order resonances. Fig. 4(b) and (c) also show the results obtained for the radially fixed inner boundary and free inner boundary. Among the three inner constraints, the radially fixed inner boundary obtains the most favorable concealing effect (Fig. 4(b)), where all of the resonant peaks are narrow and they can be suppressed well by damping. For the free inner boundary (Fig. 4(c)), a very wide resonance extends through the entire frequency range and significantly degrades the

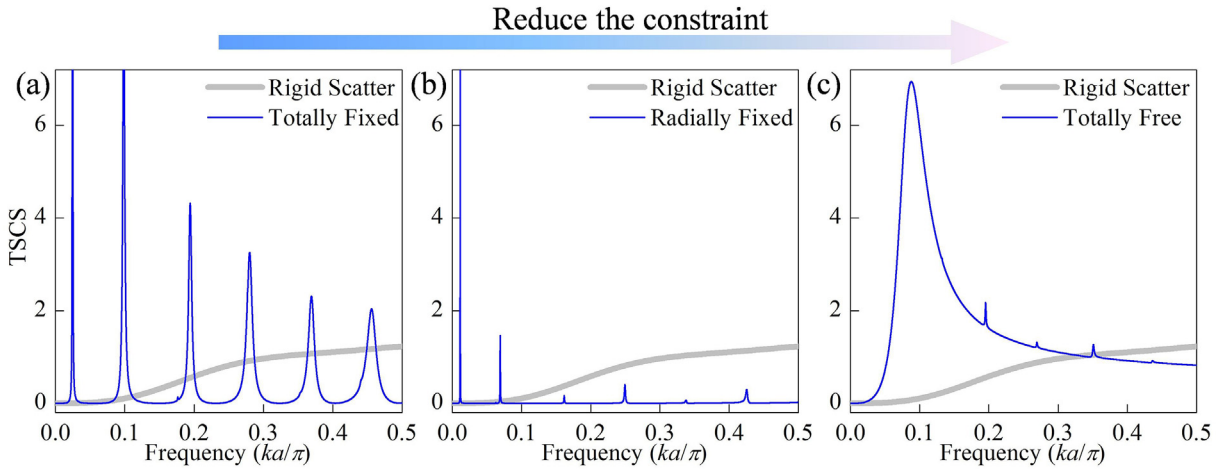


Fig. 4. TSCS for a damped cloak (damping ratio 0.5%) with (a) totally fixed inner surface, (b) radially fixed inner surface, and (c) free inner surface.

cloaking effect. This resonance is induced by the zeroth order wave and it is independent of the shear modulus. This type of resonance has also been observed in an acoustic cloak with anisotropic density meta-fluids [43].

4.3. Practical inner constraint imposed by a liner solid shell

In practice, the most convenient inner constraint for the PM cloak is the free one. However, its cloaking effect is the worst due to the strong zeroth order scattering. Thus, we propose to support the PM cloak with a solid shell on its inner surface (Fig. 5(a)). The cloak and shell are assumed to be perfectly bonded and the inner surface of the shell is assumed to be free. As a consequence, the constraint strength on the inner side of the PM cloak can be tuned continuously by varying the supporting shell thickness, thereby providing a highly practical inner constraint and giving further insights into the boundary constraint.

The cloak parameters and material damping are considered to be the same as those used above, where the shell has a thickness of d and it is made of steel (density $\rho_{\text{steel}} = 7800 \text{ kg/m}^3$, Young's modulus $E_{\text{steel}} = 220 \text{ GPa}$ and Poisson's ratio $\nu_{\text{steel}} = 0.28$). Fig. 5(b) shows the averaged TSCS versus the shell thickness. The averaged TSCS is estimated over the frequency range of $ka/\pi = 0-0.5$. For the cloak supported by a very thin shell, the averaged TSCS is close to that for a cloak with a free inner boundary. After increasing the shell thickness, excellent cloaking performance is observed for the range of $d/a = 0.005-0.01$ in a similar manner to a radially fixed inner surface. Further increasing the shell thickness increases the constraint strength and the TSCS approaches that for a cloak with a totally fixed inner surface. The TSCS for a PM cloak without/with a shell is also plotted in Fig. 5(c). For the cloak supported with an appropriate shell, all of the resonances are suppressed well by the material damping, as one expect.

It should be noted that for the free inner boundary, we assume that the shell cavity is a void with no pressure radiation into the cavity. In practical applications, it is more natural to assume that the inner cavity is filled by air. Owing to the very large impedance mismatch (10^4 orders of magnitude) between air and the PM, we anticipate that the pressure radiation into the air-filled cavity will be negligible, and thus the result will not be affected greatly in the low frequency range. To support our assumption, we theoretically and numerically investigated the case where the shell cavity is filled with air (density $\rho_{\text{air}} = 1.29 \text{ kg/m}^3$, and sound velocity $c_{\text{air}} = 343 \text{ m/s}$). The TSCS for a cloak where the shell cavity is filled with air overlaps with the case of a stress-free shell (Fig. 5(c)), and the results indicate a small impact of the inner radiation. Fig. 6 shows the simulated pressure fields for the three cases. As expected, the acoustic pressure intensity inside the cavity (Fig. 6(c)) is negligible, and the scattering has been significantly reduced by the shell (Fig. 6(b) (c)) compared with the cloak without a shell (Fig. 6(a)).

We verify this strategy for virtually tuning the inner constraint on the microstructures PM acoustic cloak. We improve our previously designed microstructure cloak by attaching a supporting steel shell to its inner surface (Fig. 7(a)). The PM cloak is constructed completely from PM unit cells (Fig. 7(b)) by optimizing the geometry parameters to match the required PM properties. The density and bulk modulus (Fig. 7(c)) are good approximations to the required continuous material parameters. The design procedure is described in detail in our previous study [19]. The shell thickness and material damping are the same as those employed above. Fig. 7(d) shows the simulated TSCS for the cloak with/without a shell, which demonstrates that excellent broadband cloaking performance is achieved with the supporting shell. Similar to the case described above, the radiation into the cavity is negligible (Fig. 7(f)) when the shell cavity is filled with air, and the cloaking effect is still preserved.

In addition to the inner constraint considered above, another important factor that affects practical applications is how to reduce the cloak's size. The cloak considered in this study has a thickness equal to its inner radius, which is clearly unacceptable for cloaking large targets. To address this issue, PMs can be designed with steeper moduli and anisotropy, or by

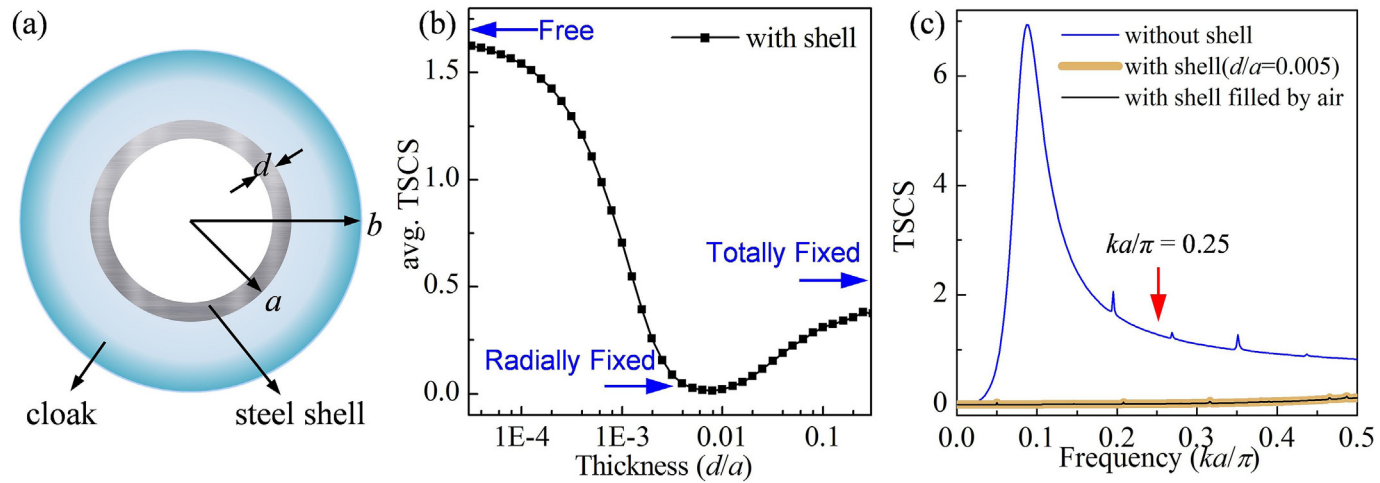


Fig. 5. Cloak supported by a traction-free inner shell; (a) Schematic configuration; (b) Averaged TSCS versus the shell thickness; (c) TSCS for a cloak without/with a shell.

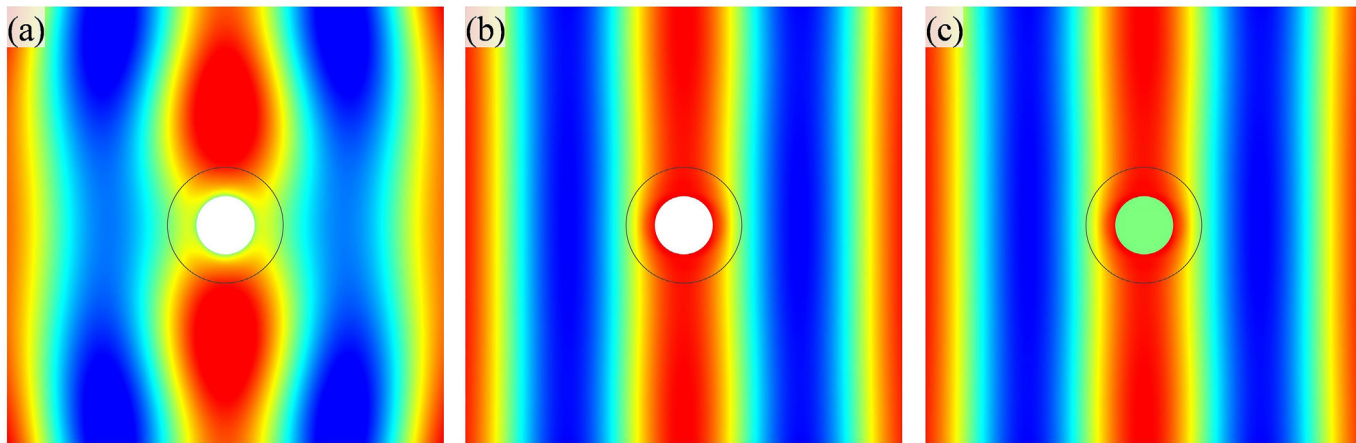


Fig. 6. Simulated cloaking performance corresponding to $ka/\pi = 0.25$. (a) Cloak without a shell; (b) Cloak with a stress-free shell; (c) Cloak with a shell cavity filled with air.

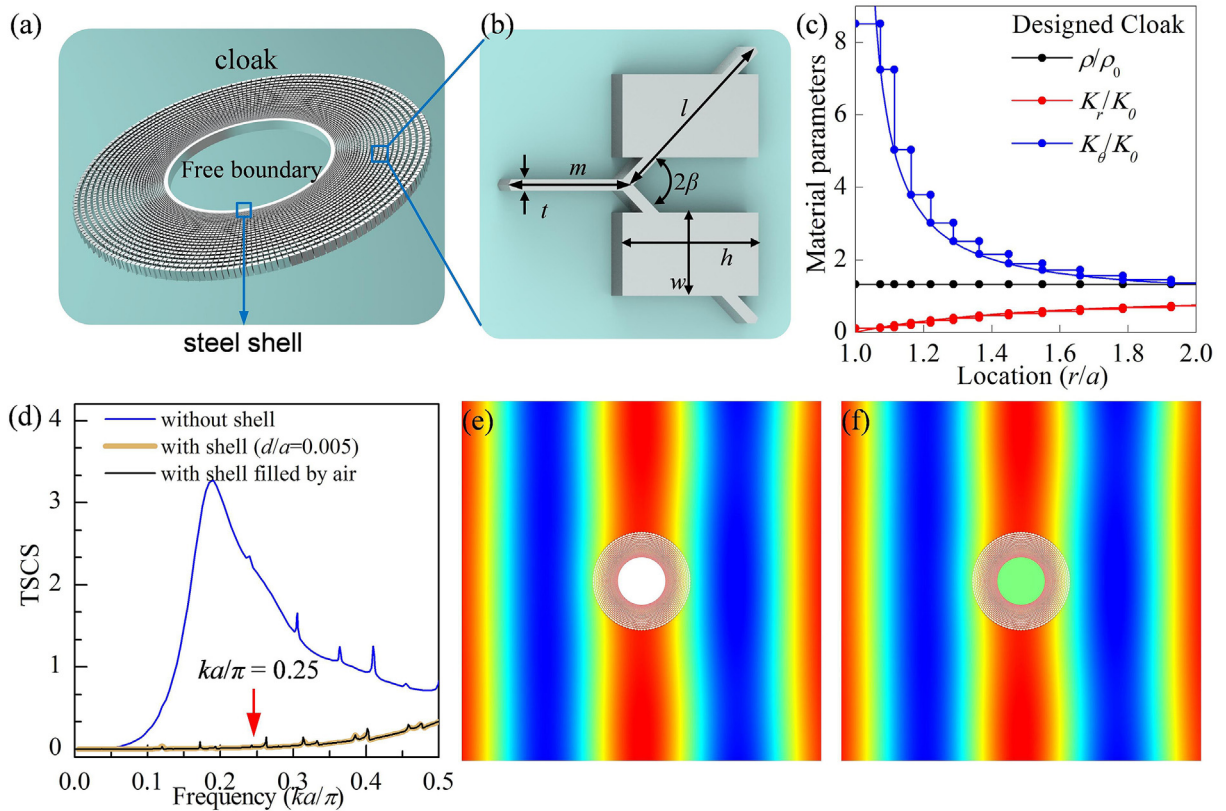


Fig. 7. Verification of the proposed boundary scheme with a microstructure PM cloak; (a) Microstructure PM cloak with an inner shell; (b) PM unit cell; (c) Distribution of material parameters; (d) TSCS for the cloak without/with a shell; Simulated cloaking performance corresponding to $ka/\pi = 0.25$ for (e) a cloak with a stress-free shell and (f) a cloak where the shell is filled with air.

optimizing the cloak parameters instead of directly using the transformation method. For instance, we have experimentally reported an optimized cloak with a thickness that is 0.4 times of its inner radius [26], where a good cloaking effect is still achieved for the targeted frequency band. We consider that the cloak's relative size can be reduced further by applying innovative techniques for PM design and cloak parameter optimization.

5. Conclusions

In this paper, a theoretical model is developed to study the scattering of a cylindrical acoustic cloak composing pentamode materials with shear rigidity, and the effects of the material parameters, damping and inner boundary constraint are systematically investigated. It is found that, shear rigidity of the pentamode materials introduces intense resonances in the low frequency range and reduces the broadband effectiveness. These resonances are explained as shear wave resonances in the radial direction, and they are essentially different from the conventional whispering-gallery resonances along the circumference. Three constraints on the cloak inner surface are examined, i.e. radially fixed, totally fixed and free inner boundary constraints. In general, the best broadband cloaking effect is achieved with the radially fixed inner constraint. For the totally fixed inner constraint, the first order resonances have large resonance widths, whereas fairly obvious zeroth order scattering is observed with the free inner constraint. To overcome the difficulty implementing a radially constrained inner boundary, we propose to attach a solid shell to the inner surface of the cloak. It is interesting to find that, the constraint strength on the cloak inner surface can be tuned continuously over the range of the three constraints by varying the shell thickness. This constraint scheme is also numerically verified with a microstructure pentamode cloak. Our findings may facilitate the implementation of pentamode cloaks by considering the pentamode imperfection, inner constraints, and broadband cloaking effectiveness.

Acknowledgements

We are grateful to A.N. Norris for discussion on resonance. This work was supported by the National Natural Science Foundation of China (Nos. 11372035, 11472044, 11632003, 11802017), Postdoctoral Innovation Talents Support Program (No. BX20180040), and the 111 Project (No. B16003).

Appendix A. Supplementary data

Supplementary data to this article can be found online at <https://doi.org/10.1016/j.jsv.2019.06.005>.

References

- [1] J.B. Pendry, D. Schurig, D.R. Smith, Controlling electromagnetic fields, *Science* 312 (2006) 1780–1782.
- [2] U. Leonhardt, Optical conformal mapping, *Science* 312 (2006) 1777–1780.
- [3] H.Y. Chen, C.T. Chan, Acoustic cloaking in three dimensions using acoustic metamaterials, *Appl. Phys. Lett.* 91 (2007) 183518.
- [4] S.A. Cummer, D. Schurig, One path to acoustic cloaking, *New J. Phys.* 9 (2007) 45.
- [5] A.N. Norris, Acoustic cloaking theory, *Proc. Math. Phys. Eng. Sci.* 464 (2008) 2411–2434.
- [6] Y. Cheng, F. Yang, J.Y. Xu, X.J. Liu, A multilayer structured acoustic cloak with homogeneous isotropic materials, *Appl. Phys. Lett.* 92 (2008) 151913.
- [7] J. Christensen, F.J.G. de Abajo, Anisotropic metamaterials for full control of acoustic waves, *Phys. Rev. Lett.* 108 (2012) 124301.
- [8] A.P. Liu, R. Zhu, X.N. Liu, G.K. Hu, G.L. Huang, Multi-displacement microstructure continuum modeling of anisotropic elastic metamaterials, *Wave Motion* 49 (2012) 411–426.
- [9] G.W. Milton, J.R. Willis, On modifications of Newton's second law and linear continuum elastodynamics, *Proc. Math. Phys. Eng. Sci.* 463 (2007) 855–880.
- [10] D. Torrent, J. Sanchez-Dehesa, Anisotropic mass density by radially periodic fluid structures, *Phys. Rev. Lett.* 105 (2010) 174301.
- [11] B.I. Popa, W. Wang, A. Konneker, S.A. Cummer, C.A. Rohde, Anisotropic acoustic metafluid for underwater operation, *J. Acoust. Soc. Am.* 139 (2016) 3325–3331.
- [12] B. Popa, L. Zigoneanu, S.A. Cummer, Experimental acoustic ground cloak in air, *Phys. Rev. Lett.* 106 (2011) 253901.
- [13] L. Zigoneanu, B. Popa, S.A. Cummer, Three-dimensional broadband omnidirectional acoustic ground cloak, *Nat. Mater.* 13 (2014) 352–355.
- [14] G.W. Milton, A.V. Cherkhev, Which elasticity tensors are realizable? *J. Eng. Mater. Technol.* 117 (1995) 483–493.
- [15] N.H. Gokhale, J.L. Cipolla, A.N. Norris, Special transformations for pentamode acoustic cloaking, *J. Acoust. Soc. Am.* 132 (2012) 2932–2941.
- [16] Y. Chen, X. Liu, G. Hu, Design of arbitrary shaped pentamode acoustic cloak based on quasi-symmetric mapping gradient algorithm, *J. Acoust. Soc. Am.* 140 (2016) L405–L409.
- [17] A. Zhao, Z. Zhao, X. Zhang, X. Cai, L. Wang, T. Wu, H. Chen, Design and experimental verification of a water-like pentamode material, *Appl. Phys. Lett.* 110 (2017) 11907.
- [18] X. Cai, L. Wang, Z. Zhao, A. Zhao, X. Zhang, T. Wu, H. Chen, The mechanical and acoustic properties of two-dimensional pentamode metamaterials with different structural parameters, *Appl. Phys. Lett.* 109 (2016) 131904.
- [19] Y. Chen, X.N. Liu, G.K. Hu, Latticed pentamode acoustic cloak, *Sci Rep-Uk* 5 (2015) 15745.
- [20] Y. Tian, Q. Wei, Y. Cheng, Z. Xu, X.J. Liu, Broadband manipulation of acoustic wavefronts by pentamode metasurface, *Appl. Phys. Lett.* 107 (2015) 221906.
- [21] C.N. Layman, C.J. Naify, T.P. Martin, D.C. Calvo, G.J. Orris, Highly anisotropic elements for acoustic pentamode applications, *Phys. Rev. Lett.* 111 (2013) 24302.
- [22] J. Cipolla, N. Gokhale, A. Norris, A. Nagy, Design of inhomogeneous pentamode metamaterials for minimization of scattering, *J. Acoust. Soc. Am.* 130 (2011) 2332.
- [23] C.L. Scandrett, J.E. Boisvert, T.R. Howarth, Broadband optimization of a pentamode-layered spherical acoustic waveguide, *Wave Motion* 48 (2011) 505–514.
- [24] C.L. Scandrett, J.E. Boisvert, T.R. Howarth, Acoustic cloaking using layered pentamode materials, *J. Acoust. Soc. Am.* 127 (2010) 2856–2864.
- [25] A.C. Hladky-Hennion, J.O. Vasseur, G. Haw, C. Croenne, L. Haumesser, A.N. Norris, Negative refraction of acoustic waves using a foam-like metallic structure, *Appl. Phys. Lett.* 102 (2013) 144103.
- [26] Y. Chen, M. Zheng, X. Liu, Y. Bi, Z. Sun, P. Xiang, J. Yang, G. Hu, Broadband solid cloak for underwater acoustics, *Phys. Rev. B* 95 (2017).
- [27] Z. Sun, H. Jia, Y. Chen, Z. Wang, J. Yang, Design of an underwater acoustic bend by pentamode metafluid, *J. Acoust. Soc. Am.* 3 (2018) 1029–1034.
- [28] A. Martin, M. Kadic, R. Schittny, T. Bückmann, M. Wegener, Phonon band structures of three-dimensional pentamode metamaterials, *Phys. Rev. B* 86 (2012) 155116.
- [29] M. Kadic, T. Bückmann, N. Stenger, M. Thiel, M. Wegener, On the practicability of pentamode mechanical metamaterials, *Appl. Phys. Lett.* 100 (2012) 191901.
- [30] M. Kadic, T. Bückmann, R. Schittny, M. Wegener, On anisotropic versions of three-dimensional pentamode metamaterials, *New J. Phys.* 15 (2013).
- [31] M. Kadic, T. Bückmann, R. Schittny, P. Gumbsch, M. Wegener, Pentamode metamaterials with independently tailored bulk modulus and mass density, *Phys Rev Appl* 2 (2014) 54007.
- [32] Y. Huang, X.G. Lu, G.Y. Liang, Z. Xu, Pentamodal property and acoustic band gaps of pentamode metamaterials with different cross-section shapes, *Phys. Lett.* 380 (2016) 1334–1338.
- [33] A. Amendola, G. Benzoni, F. Fraternali, Non-linear elastic response of layered structures, alternating pentamode lattices and confinement plates, *Composites Part B* 115 (2017) 117–123.
- [34] F. Fraternali, A. Amendola, Mechanical modeling of innovative metamaterials alternating pentamode lattices and confinement plates, *J. Mech. Phys. Solids* 99 (2017) 259–271.
- [35] M. Zheng, Y. Chen, X. Liu, G. Hu, Two-dimensional water acoustic waveguide based on pressure compensation method, *Rev. Sci. Instrum.* 89 (2018) 24902.
- [36] R. Schittny, T. Bückmann, M. Kadic, M. Wegener, Elastic measurements on macroscopic three-dimensional pentamode metamaterials, *Appl. Phys. Lett.* 103 (2013) 231905.
- [37] J.D. Smith, P.E. Verrier, The effect of shear on acoustic cloaking, *P Roy Soc a-Math Phy* 467 (2011) 2291–2309.
- [38] W.Q. Chen, Z.G. Bian, H.J. Ding, Three-dimensional vibration analysis of fluid-filled orthotropic FGM cylindrical shells, *Int. J. Mech. Sci.* 46 (2004) 159–171.
- [39] S.M. Hasheminejad, M. Rajabi, Acoustic resonance scattering from a submerged functionally graded cylindrical shell, *J. Sound Vib.* 302 (2007) 208–228.
- [40] A.S. Titovich, A.N. Norris, Tunable cylindrical shell as an element in acoustic metamaterial, *J. Acoust. Soc. Am.* 136 (2014) 1601–1609.
- [41] A.N. Norris, Resonant acoustic scattering from solid targets, *J. Acoust. Soc. Am.* 88 (1990) 505–514.
- [42] L. Flax, L.R. Dragonette, H. Überall, Theory of elastic resonance excitation by sound scattering, *J. Acoust. Soc. Am.* 63 (1978) 723–731.
- [43] Y. Cheng, X.J. Liu, Resonance effects in broadband acoustic cloak with multilayered homogeneous isotropic materials, *Appl. Phys. Lett.* 93 (2008) 71903.